General Disclaimer

One or more of the Following Statements may affect this Document

- This document has been reproduced from the best copy furnished by the organizational source. It is being released in the interest of making available as much information as possible.

- This document may contain data, which exceeds the sheet parameters. It was furnished in this condition by the organizational source and is the best copy available.

- This document may contain tone-on-tone or color graphs, charts and/or pictures, which have been reproduced in black and white.

- This document is paginated as submitted by the original source.

- Portions of this document are not fully legible due to the historical nature of some of the material. However, it is the best reproduction available from the original submission.

Produced by the NASA Center for Aerospace Information (CASI)

A MODEL FOR SILICON SOLAR CELL PERFORMANCE IN SPACE

FINAL REPORT

by

M. J. Barrett and R. H. Stroud

February 28, 1969

JPL Contract 952246

with

EXOTECH INCORPORATED
Systems Research Division
525 School Street, S.W.
Washington, D.C. 20024

FACILITY FORM 602

N69-24389
(ACCESSION NUMBER)

46
(PAGES)

CR 100776
(NASA CR OR TMX OR AD NUMBER)

(THRU)
1

(CODE)
03

(CATEGORY)

A MODEL FOR SILICON SOLAR CELL PERFORMANCE IN SPACE

FINAL REPORT

by

M. J. Barrett and R. H. Stroud

February 28, 1969

JPL Contract 952246

This work was performed for the Jet Propulsion Laboratory, California Institute of Technology, as sponsored by the National Aeronautics and Space Administration under Contract NAS7-100.

This report contains information prepared by Exotech Incorporated under JPL subcontract. Its content is not necessarily endorsed by the Jet Propulsion Laboratory, California Institute of Technology, or the National Aeronautics and Space Administration.

ABSTRACT

Results of a study of the parameters affecting silicon solar cell performance in space are presented. Comparison of semiconductor theory, radiation effects theory, and reported experimental data has permitted development of a mathematical model for predicting the performance of a solar cell under combinations of radiation exposure, ambient temperature, and illumination spectrum. Limitations on the accuracy and applicability of the model are discussed for future study.

TABLE OF CONTENTS

INTRODUCTION AND SUMMARY 1

I. MODEL OF THE SOLAR CELL 3
- A. Solar Cell Equation 3
- B. Photovoltaic Current I_L 6
- C. Diode Characteristics 13
- D. Cell Resistance 16

II. OPTICAL EFFECTS 17
- A. Coverslide Transmission 17
- B. Absorption in Silicon 19
- C. Coverslide Darkening. 19

III. RADIATION EFFECTS 22
- A. Proton Shielding. 22
- B. Proton Damage 24
- C. Electron Shielding. 26
- D. Electron Damage 28

IV. RECOMMENDED FUTURE WORK 30
- A. Low Energy Proton Damage. 30
- B. Resistance Effects. 34

V. GLOSSARY. 35

VI. REFERENCES. 39

VII. NEW TECHNOLOGY. 41

APPENDIX. 41

INTRODUCTION AND SUMMARY

A mathematical technique or model for quantitative prediction of the electrical output of solar cells is an obvious asset in the design, selection, and performance prediction of a spacecraft power system. Laboratory measurements can provide this information for solar cell assemblies from the manufacturer. The technique described in this report permits an extrapolation of these measurements to the future output when aboard a spacecraft in space.

The model has been developed after study of the extensive literature available. Insomuch as practicable, it adheres to basic physical theory, since no empirical scheme has been presented so far which is capable of including such diverse effects as nonuniform proton damage or the interaction of a degraded solar cell with slant sunlight.

This report presents the equations of the model and a discussion of their origin, meaning, and implications. A complete calculation would follow the flow chart outlined on the next page. In this chart, boxes represent major derived quantities. The input parameters necessary for each derivation are listed alongside the arrows leading to the boxes; these parameters are defined in the Glossary. The numbers in parentheses refer to the appropriate numbered equations in the text. (We are indebted to Mr. Paul Berman for suggesting this display.)

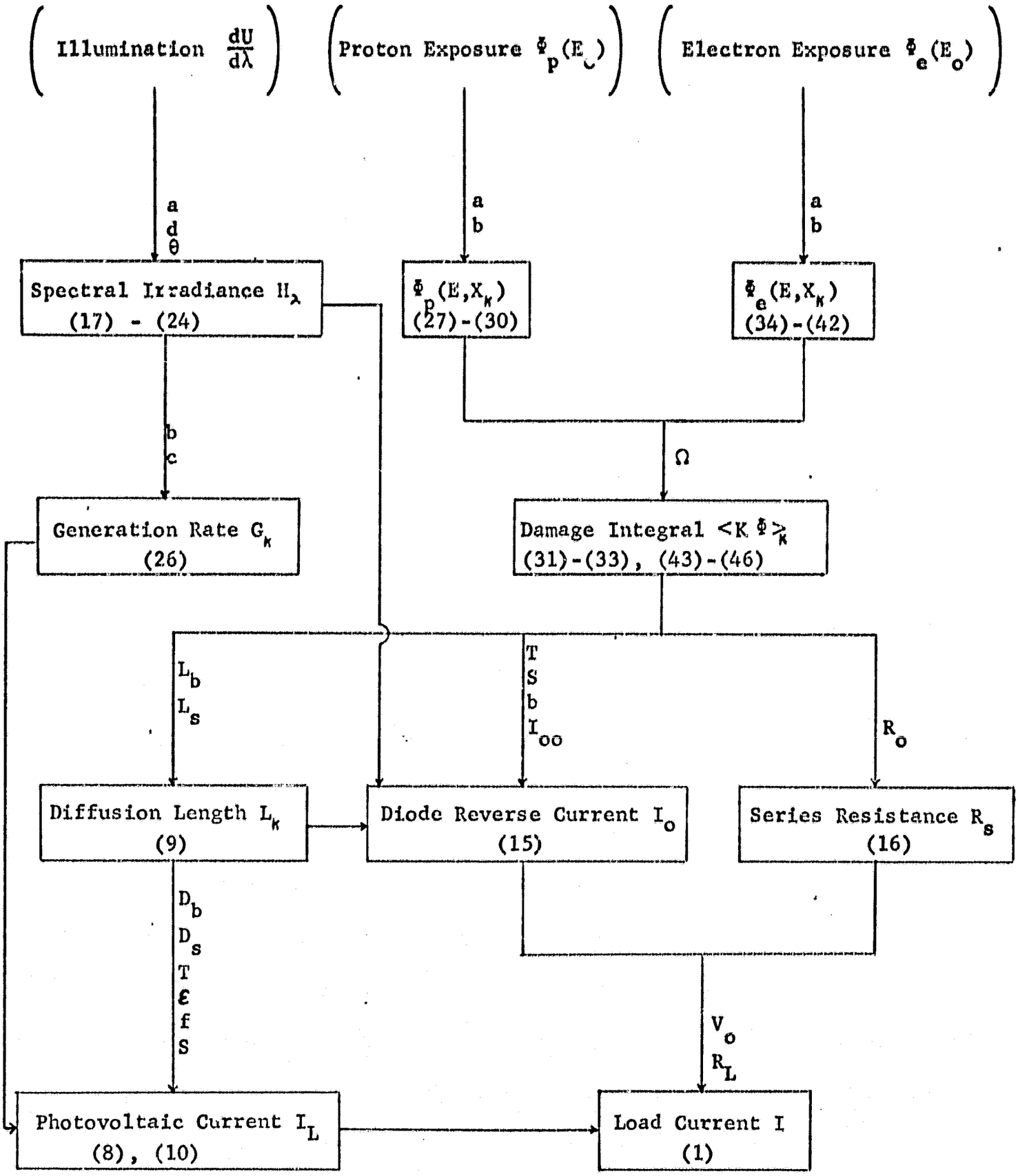

Flow chart for mathematical model. The quantities in boxes are calculated from the previous boxes and the input variables on the flow lines. Symbols are defined in the Glossary.

I. MODEL OF THE SOLAR CELL

A. Solar Cell Equation

The physically observable parameters of a silicon solar cell are its area S, its thickness b, and the fraction f of its front surface area which is not covered by the metallic contact grid and bus bar. A transparent coverslide is generally placed over the cell, and its thickness will be denoted as a.

The general optical and electrical properties of the solar cell can be described by several other parameters. The transmission of light of wavelength λ through its surface, or the assembly when a coverslide is present, will be denoted as t_λ. The absorption of the same light by an incremental thickness dx of solar cell will be denoted as α_λ. Both transmission and absorption depend not only on wavelength but also on the angle of incidence. Electrically, the cell exhibits a junction depth x_j which separates a surface region, generally of n-type silicon, from a base region of the opposite polarity. Some resistance R_s is observed between the front and back connections.

Observing that a solar cell acts as a diode operating in opposition to a current source, Prince and Wolf proposed the solar cell equation (ref. 1). Our only change to this equation is to replace the usual expression AKT/q by the single parameter V_o. We propose calling V_o the "characteristic voltage" of the solar cell, and write the equation as

$$I = I_L - I_o \left[e^{I(R_L + R_s)/V_o} - 1 \right] \qquad (1)$$

A reasonable question is whether the solar cell equation can be expected to reproduce the current-voltage curve of a solar cell that has been heavily degraded by radiation, and perhaps degraded in a nonuniform manner. To test the possibility of fit to such a cell, a series of experimental curves by Lodi (ref. 2) and by Statler and Curtin (ref. 3) have been analyzed. An iterative selection of R_s, V_o, the photovoltaic current I_L, and the reverse diode current I_o leads to the fits which are presented as Figures 1 and 2. These fits seem adequate for engineering use, and indicate

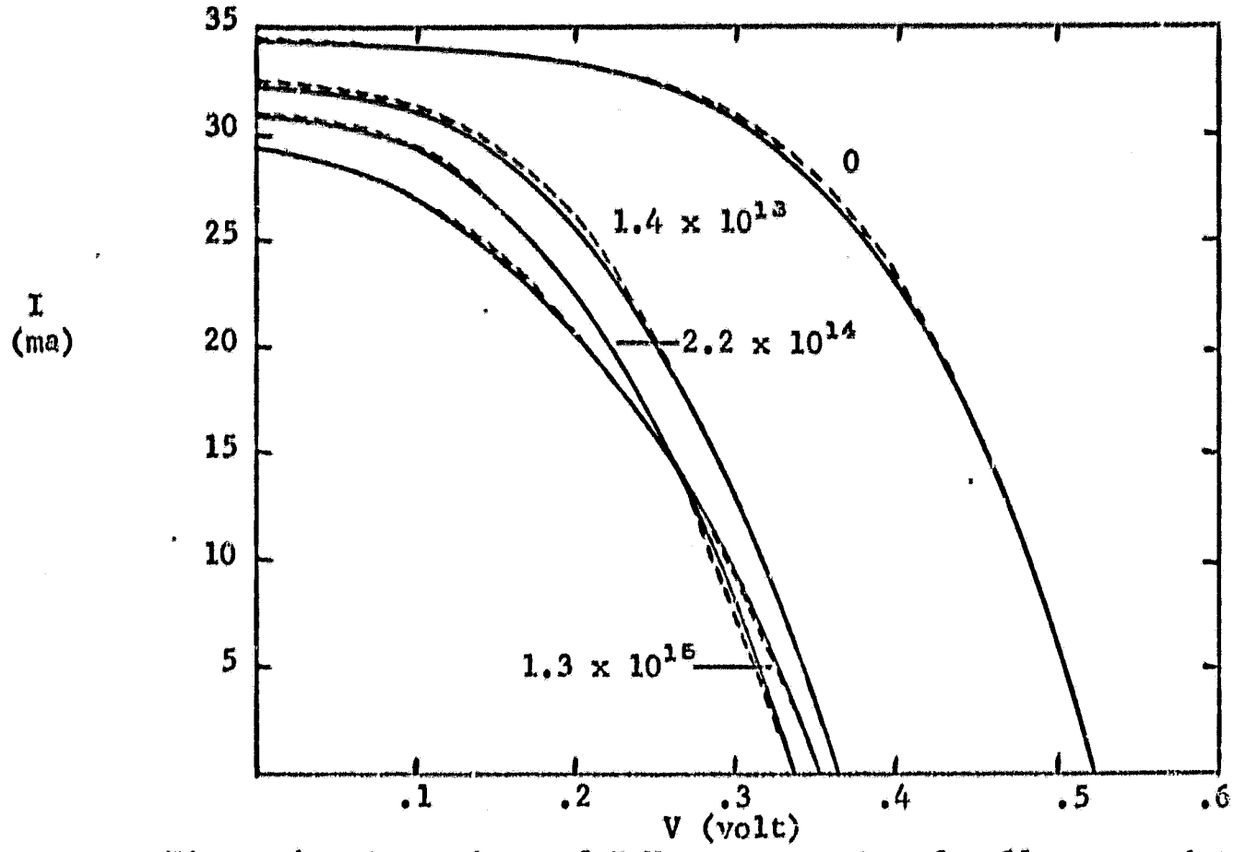

Figure 1. Comparison of I-V measurements of cells exposed to fluence of 100 keV protons (solid line from ref. 2) with empirical fits of the solar cell equation (dashed line).

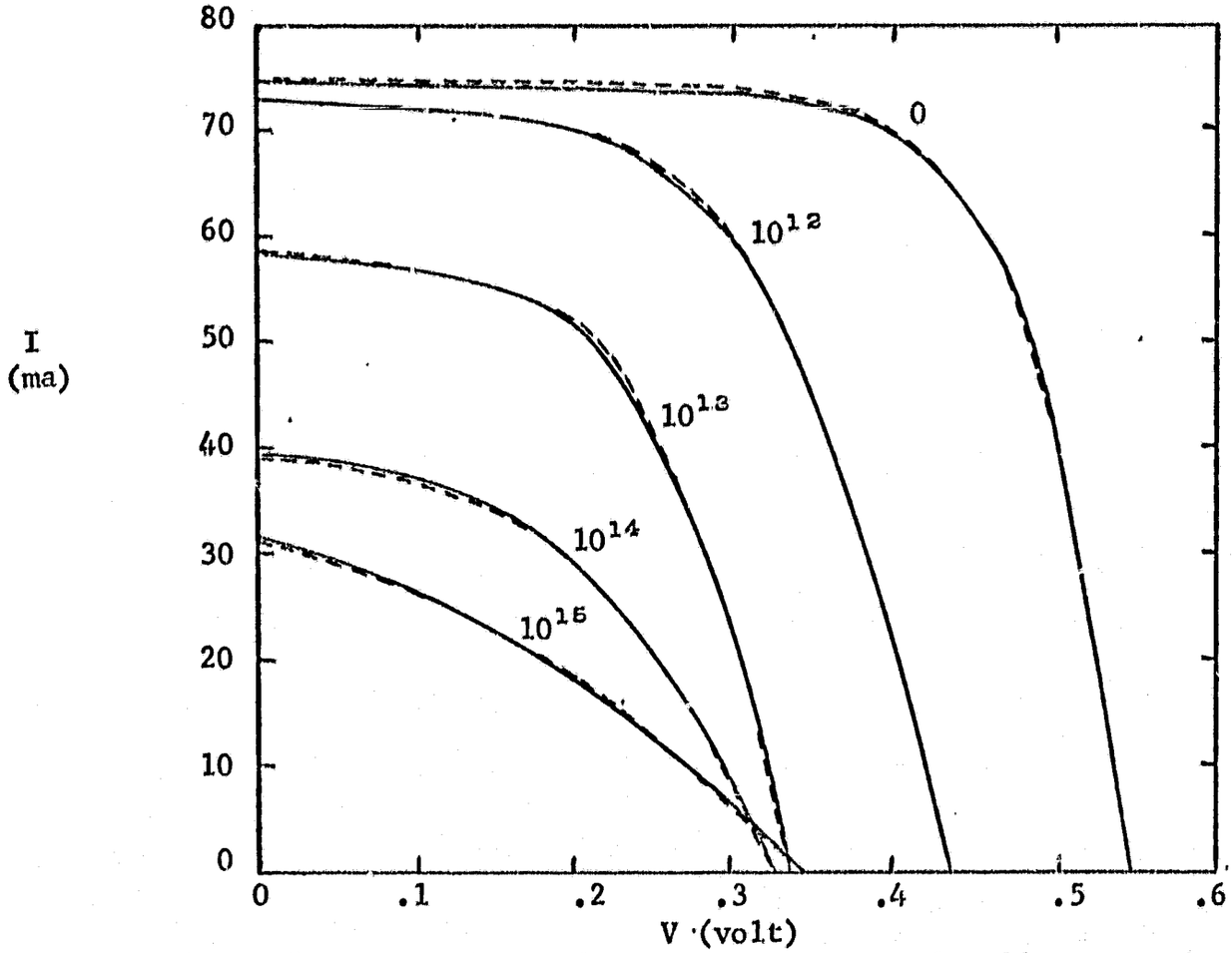

Figure 2. Comparison of I-V measurements of cells exposed to fluences of 270 keV protons (solid line, from ref. 3) with empirical fits of the solar cell equation (dashed line).

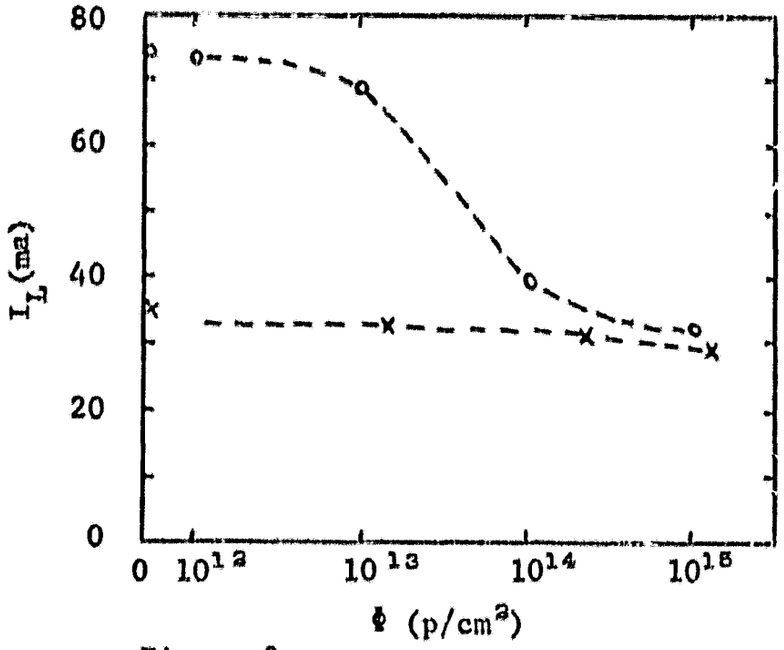

Figure 3.

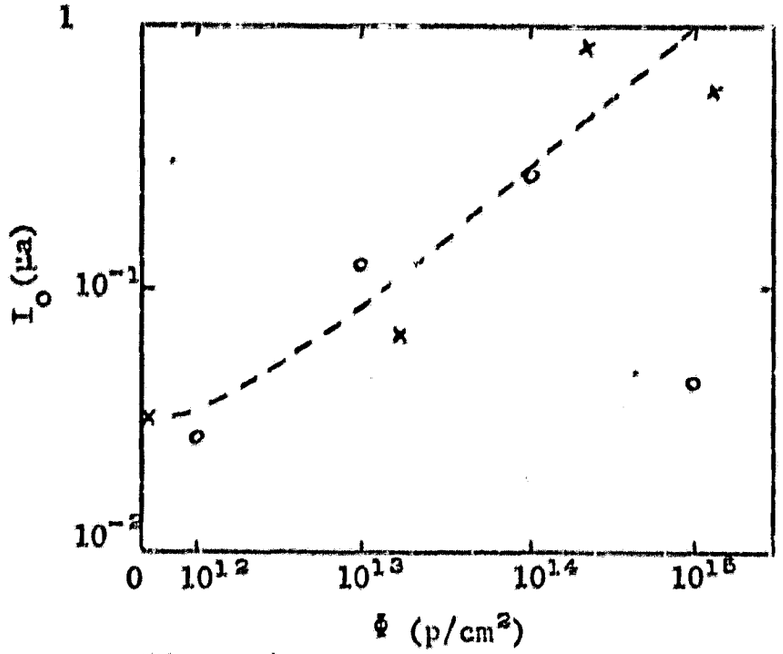

Figure 4.

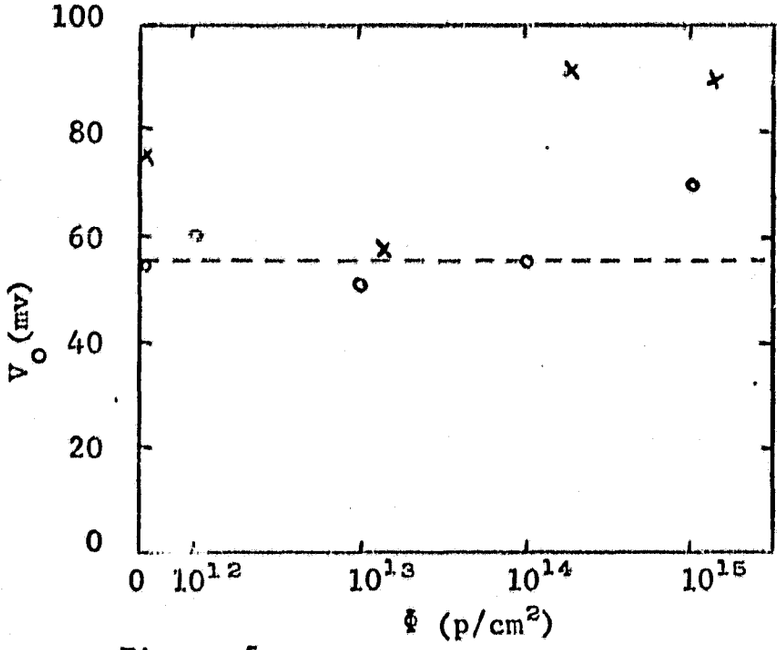

Figure 5.

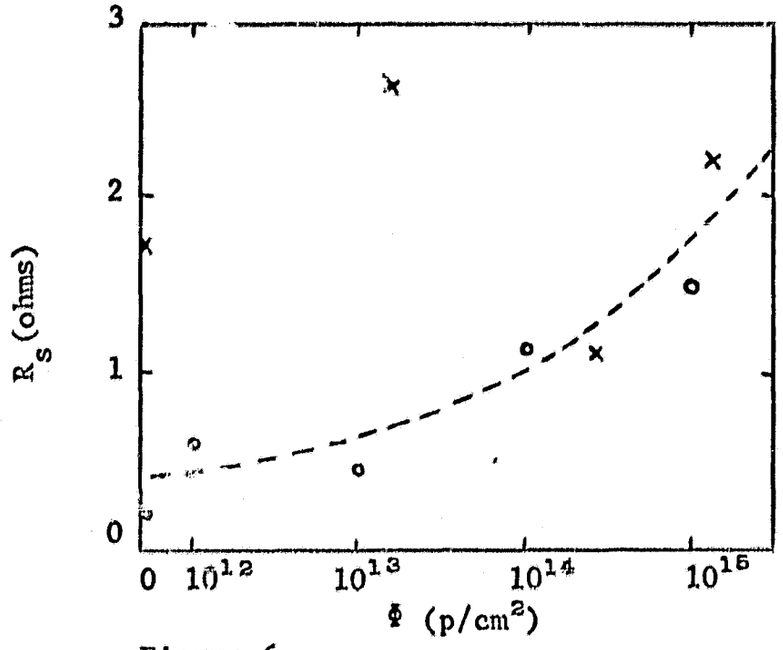

Figure 6.

Empirical constants used in the solar cell equation to generate the fits shown in Figure 1 (crosses) and 2 (circles). The dashed lines suggest possible trends in the parameters with increasing exposure Φ to protons.

that indeed the solar cell equation can describe even highly damaged cells. This could be anticipated on theoretical grounds: the concepts of a diode junction and a current-producing region on each side are still present even in a highly damaged cell. The absence of a shunt resistance* is not anticipated in theory, but further analysis of these curves indicates it is absent here. Shunts have been invoked to analyze damage to solar cells with coverslides that partially expose the silicon surface (ref. 4).

The parameters of the solar cell equation used for these fits of the measured solar cell outputs are presented in Figures 3 through 6, as functions of exposure of the cell to low energy protons. Similar success in use of the solar cell equation is obtained for undamaged cells and for cells that have been damaged more uniformly, as by electron exposure.

B. Photovoltaic Current I_L

The photovoltaic current is that current across the junction due to generation by light of minority charge carriers in the solar cell. The total current from a solar cell equals I_L less that current that returns across the junction due to its action as a diode. Thus, I_L is proportional to light intensity but this does not follow for the total current.

The short-circuit current I_{sc} approximates the photovoltaic current I_L for silicon solar cells with typically negligible resistance.

The photovoltaic current is simply the photovoltaic current density j multiplied by the area of the solar cell that is exposed to the light source. This is somewhat less than the actual front surface area, inasmuch as the front contact typically covers 10% of the total surface. The continuity equation implies that j is also proportional to the light intensity U for a given spectrum.

The equations necessary for determination of j are the continuity equation

$$\frac{1}{q}\,\frac{dj}{dx} - \frac{n(x)}{\tau(x)} + G(x) = 0 \qquad (2)$$

*That is, an open-circuit in lieu of a resistance element across the equivalent circuit (ref. 1) of a solar cell. Our model is in agreement with that given in ref. 18.

the current equation

$$j = q D \frac{dn}{dx} + q \mu E n \qquad (3)$$

the dc equation

$$\frac{1}{L^2} = \frac{1}{L_o^2} + K \Phi \qquad (4)$$

the diffusion relation

$$L^2 = \tau D \qquad (5)$$

and the Einstein relation

$$q D = \mu k T \qquad (6)$$

Combining the continuity and current equations eliminates j. Furthermore, it may be assumed that D and E are constant through the region being considered. The resulting expression may be written as a difference equation

$$D\left[n_{k+1} - 2n_k + n_{k-1}\right] + \mu E h \left[n_k - n_{k-1}\right] - n_k h^2 / \tau_k + G_k h^2 = 0 \qquad (7)$$

where the continous differential equation is approximated by using discrete values of n for points of the independent variable x spaced a distance h apart. (Thus, n_k is the magnitude of n at a distance k h from the junction.)

Grouping the expressions gives a formula for progression in the solution of n_k. After elimination of μ by the Einstein relation and τ by the diffusion relation, the formula becomes

$$n_{k+1} = (2 - q E h / k T + h^2/L_k^2)\, n_k + (q E h / k T - 1)\, n_{k-1} - G_k h^2 / D \qquad (8)$$

Radiation damage affects the solution to this formula principally by decreasing L_k^2 according to the damage equation

$$\frac{1}{L_k^2} = \frac{1}{L_o^2} + \langle K \Phi \rangle_k \qquad (9)$$

where the particle fluence to which an incremental volume of the cell (at depth x_k) is exposed becomes an integral over all particle energies. When there are several types of particles (electrons, protons, alpha particles, etc.) there will be a sum of several integrals.

The assumptions are made here that any change in D is negligible, and that the migration of the damage-induced recombination centers from their points of formation is also a negligible effect. These assumptions allow a solution of Eq. 9 to be applied directly to Eq. 8 and the carrier density n_k to be developed.

The field E will be shown below to be proportional to temperature T. As a result, temperature enters into Eq. 8 only by increasing the diffusion coefficient in accordance with the Einstein relation. The increase in D reduces the magnitude of the negative term and leads to an increase in current with increase in temperature. The trend is in agreement with the positive temperature coefficient normally observed for the short circuit current. However, the current of solar cells not operated near short-circuit generally has a negative temperature coefficient because of diode characteristics discussed in the next section.

To solve Eq. 8, it is necessary to have values for n_o and n_1. We assume the boundary conditions that the carrier density vanishes at the junction and at the cell surface. This assumption was also made by Bullis and Runyan,[16] but other boundary conditions have been assumed. We guess n_1 and calculate all the higher values of n_k. We iterate this guessing of n_1 until we arrive at a satisfactory value for the carrier density at the cell surface.

The accuracy of the initial guess for n_1 is of importance in determining how often the calculation must be iterated before obtaining a zero carrier density at the contact surface of the cell. If the guess for

n_1 is too small, then the values of n_k determined via Eq. 8 will change sign in the cell. If it is too large, the n_k at the back of the cell will fail to be zero.

Iterating on n_1 leads to as close an estimate as is desired. One possible technique for convergence is to compare each n_k with n_{k-1} and if there is a sign change then stop, increase the estimate for n_1 by a nominal 10% and repeat. When there is no sign change, decrease the estimate for n_1 by a nominal 5% and repeat until a sign change occurs. Then increase by 1% until there is no sign change. Such a convergence routine can obviously be carried to any level of accuracy in the estimate of n, for the solar cell in question, by taking advantage of this sign change.

The current equation relates n_1 to the current from the base into the junction. Evaluating this as a difference equation at k equal zero, we have

$$j = q D n_1 / h \tag{10}$$

since the boundary condition requires that n_o vanishes. This j is the calculated photovoltaic current I_L in ampere per square centimeter, for the solar cell. For a cell with negligible internal resistance, the short-circuit current I_{sc} is j times that portion of the surface area not covered by the contact bar and grid.

Equation 8 is simplified in the base region since the electric field E is negligible in a uniformly-doped crystal. The electric field is dependent on the impurity concentration, N, through the relationship

$$E = \frac{-kT}{q} \frac{1}{N} \frac{dN}{dx} \tag{11}$$

When there is no impurity concentration gradient in the base region, Eq. 8 reduces to

$$n_{k+1} = (2 + h^2/L_k^2)\, n_k - n_{k-1} - G_k h^2 / D \tag{12}$$

The current density calculation so far has considered only the solar cell base region contribution. In order to determine the contribution by the surface region, the same procedure may be used. Since the surface region is heavily doped, and, consequently, has a relatively short minority carrier lifetime, this contribution to the total photovoltaic current density is small and often neglected. The electric field does not vanish in this region because of the dopant gradient which is the result of diffusing phosphorus into the crystal to form the p/n junction. The magnitude of the photovoltaic current contributed by the surface layer is not significantly changed unless the electric field is on the order of 10^3 volts/cm.

The minority carrier concentration for a 10 mil n/p solar cell was computed for various values of diffusion length. Figure 7 shows the results of the calculations with the base divided into 500 increments. Figure 8 shows a plot of the short-circuit current density versus diffusion length for these calculations.

To calculate I_L, the sequence is

1. The carrier generation rate G due to light absorption is obtained as a function of depth into the cell. The usual assumption is that one minority carrier is raised to the conduction band for each photon absorbed. Thus, for monochromatic light traveling at an angle θ through the silicon, $\alpha(\lambda/hc)\ U\ e^{-\alpha x/\cos\theta}\ \sec\theta\ dx$ equals the rate of generation in an increment dx at depth x, where α is the absorption coefficient for the light of wavelength λ, and (λ/hc) is the number of photons per watt of light incident.

2. From G and the minority carrier diffusion length, computed as functions of depth x into the cell, the carrier distribution is computed, using the continuity equation and the condition that n vanishes at front, back, and junction of the cell.

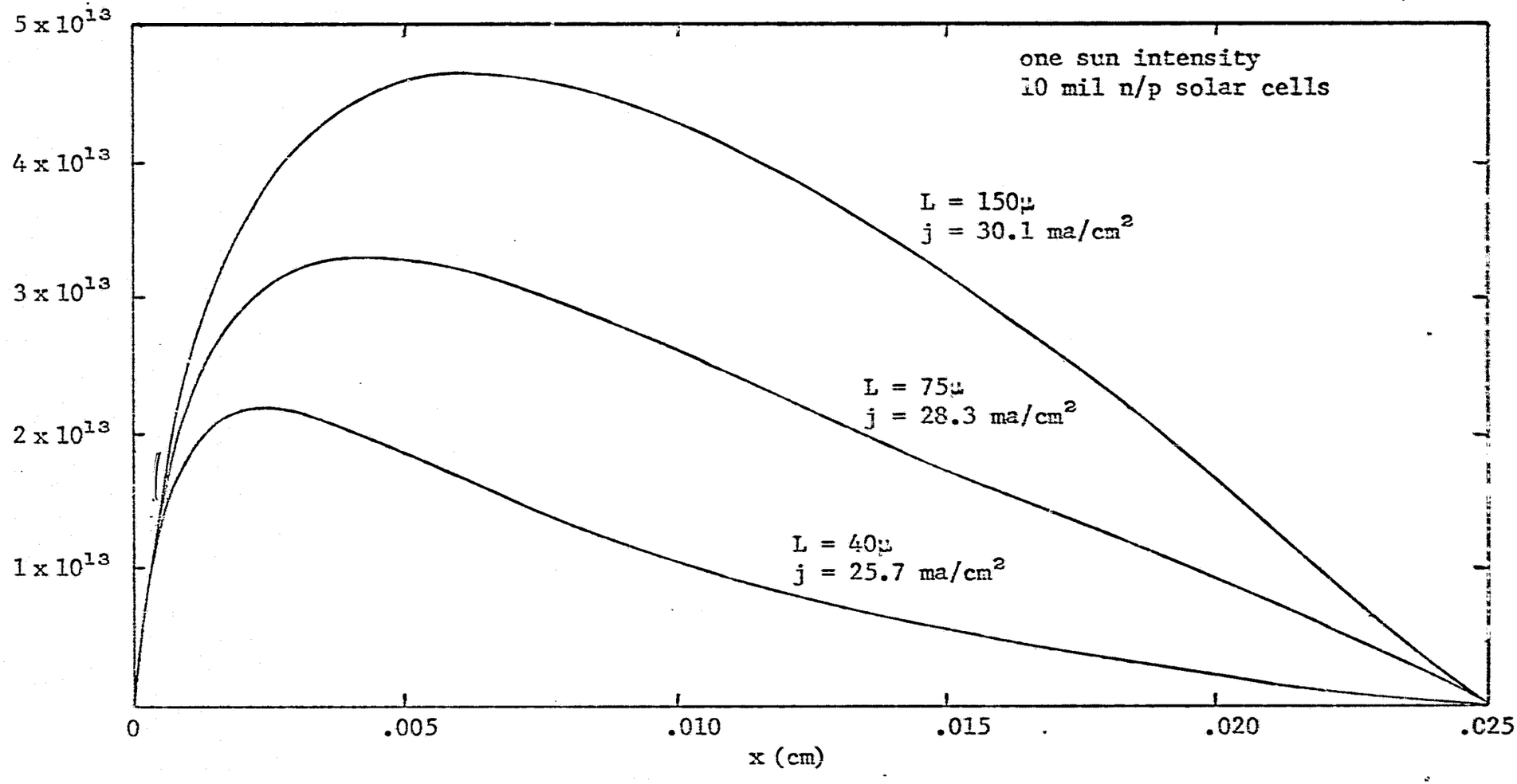

Figure 7. Minority carrier concentration (electrons/cm^3) as a function of distance from the junction in three solar cells with different values of L. These concentrations were computed using 500 intervals, and the photovoltaic current from base into junction, on each curve, was computed with Eq. 12.

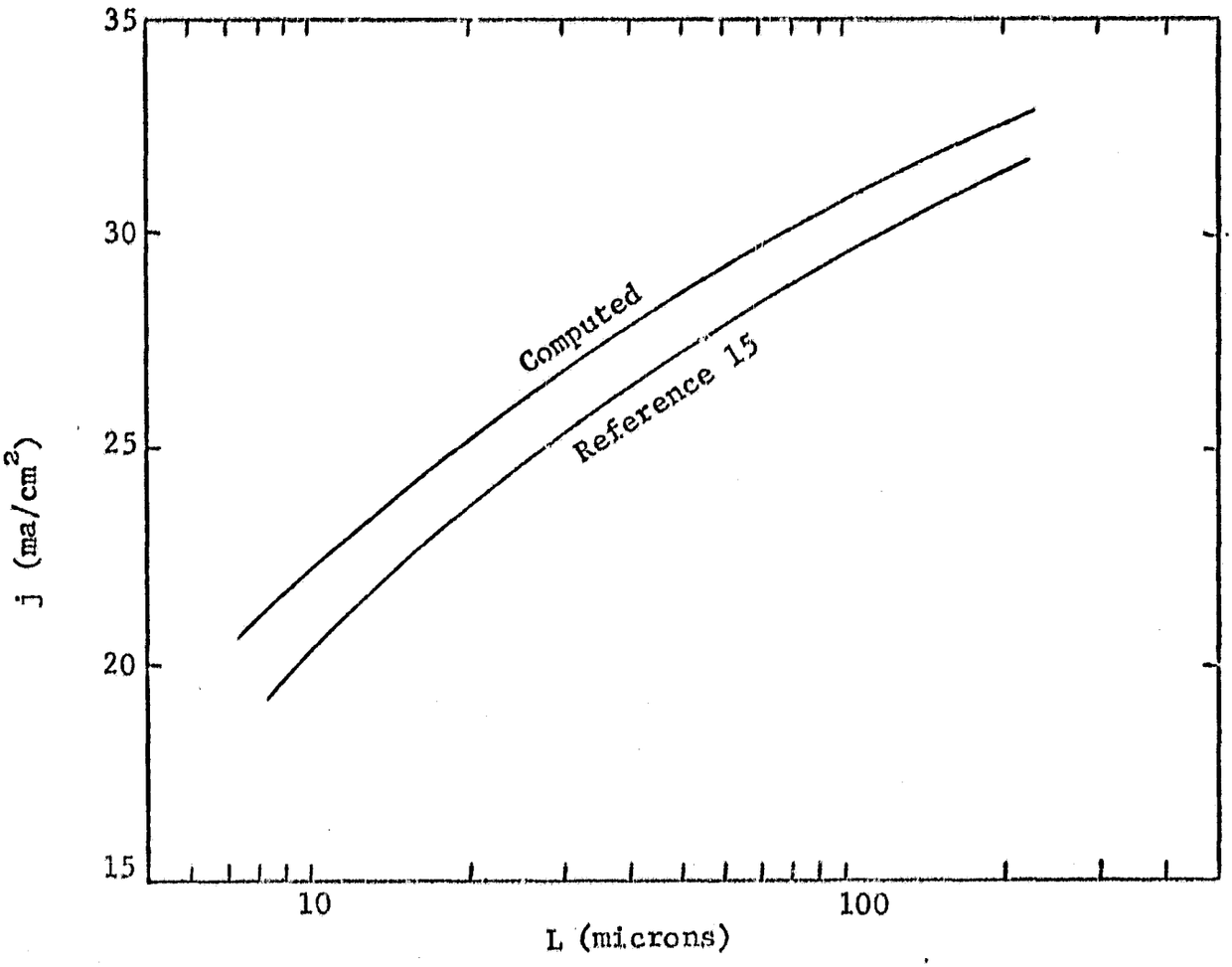

Figure 8. A comparison of computed values of photovoltaic current, versus L, with reported data from Reference 15. For the computation, the base region of a 10 mil cell was divided into 500 intervals.

3. The photovoltaic current density j is obtained from the derivatives of the minority carrier distributions on either side of the junction. Most of the contribution to j comes from the base region.

4. j is multiplied by fS to obtain I_L. This conventional step neglects edge effects in the cell, but appears to be a good approximation in our calculations so far.

When radiation reduces the minority carrier diffusion length in the base, I_L is decreased. Thus, radiation that does not penetrate far beyond the junction will affect I_L very little. This is verified by Figure 3, where I_L decreases with exposure to protons that do penetrate (270 keV), but not with exposure to the lower energy protons (100 keV) that do not penetrate greatly into the base region.

C. Diode Characteristics

Shockley's analysis (ref. 5) for diode junctions provides a theoretical expression for the diode saturation current I_o that is

$$I_o = qS\left(\frac{p\,D_p}{L_p} + \frac{n\,D_n}{L_n}\right) \qquad (13)$$

where the fractions are the product of the minority carrier concentration on either side of the junction and its diffusion coefficient, divided by its diffusion length. In an n/p solar cell, where the surface region is heavily doped, the fraction $p\,D_p/L_p$ can be neglected and I_o becomes inversely proportional to the base minority carrier diffusion length near the junction. Since L_p changes with radiation exposure in a predictable manner, a measure of the accuracy of this expression can be taken from radiation experiments. Figure 9 shows a plot of I_o calculated from various published measurements. With Downing's (ref. 6) and Luft's data (ref. 7) which did not include complete curves we have used the approximation.

$$I_o = I_{sc}e^{-Voc/Vo} \qquad (14)$$

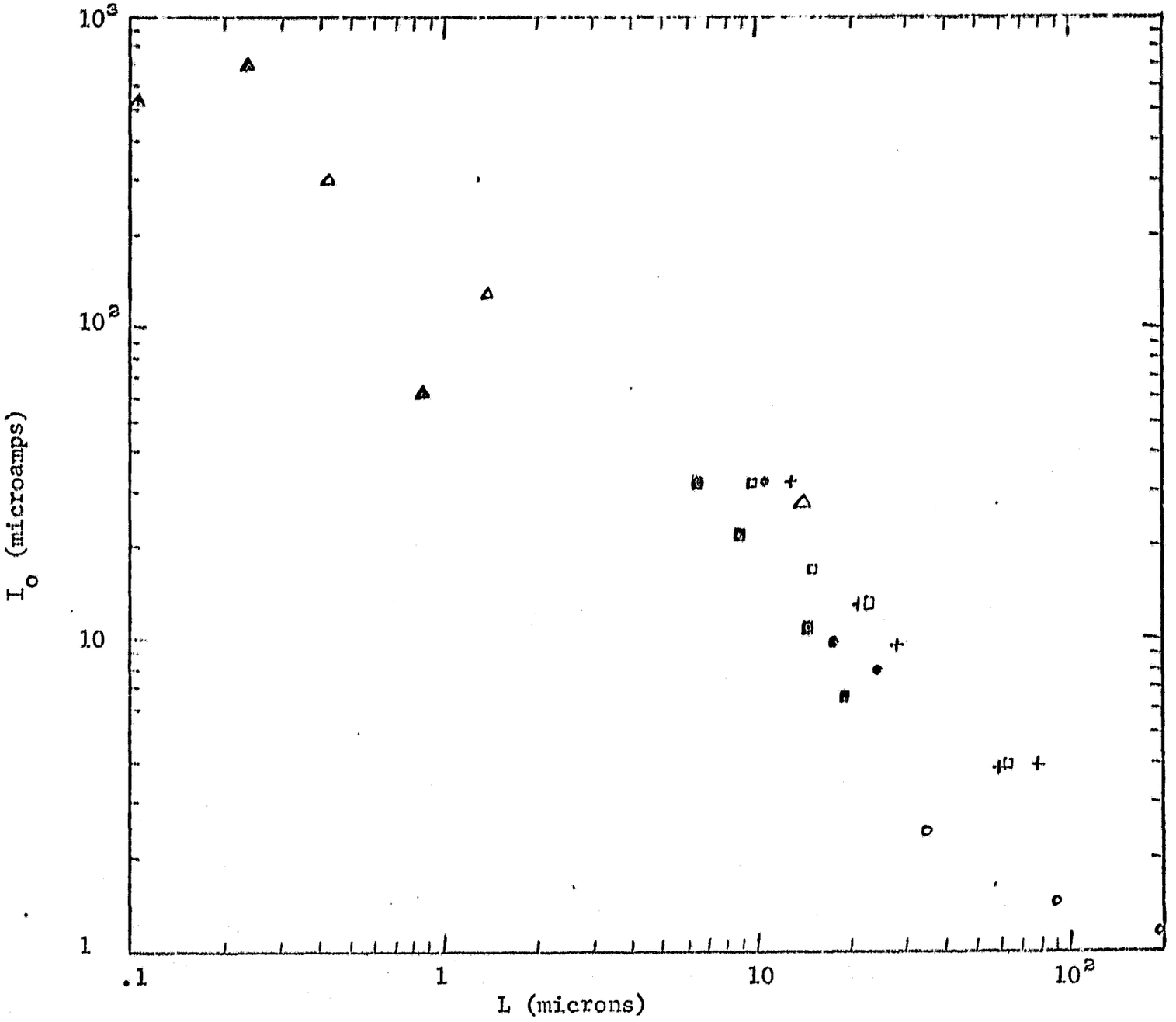

Figure 9. Calculated values of I_o from various measurements of irradiated solar showing its dependence on the reciprocal of the diffusion length L.

Δ	Statler	.27 MeV protons
▲	Lodi	.1 MeV protons
▣	Downing	.5 MeV protons
□	Downing	1 MeV protons
o	Downing	1.5 MeV protons
+	Downing	1.9 MeV protons
o	Luft	1 MeV protons

which implies negligible resistance R_s. With Statler's and Iodi's I-V curves, fits were made which included small values of R_s that increase with increasing exposure to radiation.

A similar analysis was made of data taken under variable light intensity. That I_o appears to vary as the logarithm of the light intensity U appears in Figure 10 as a result of this analysis. An equation to combine these effects with the noted dependence on L is

$$I_o = (I_{oo} + 2.21 \ell n U/U_o) e^{a(T-300)} (L_b/L_1) \qquad (15)$$

The expression for I_o is given in terms of its value I_{oo} in the initial solar cell at room temperature, illuminated at one sun intensity.

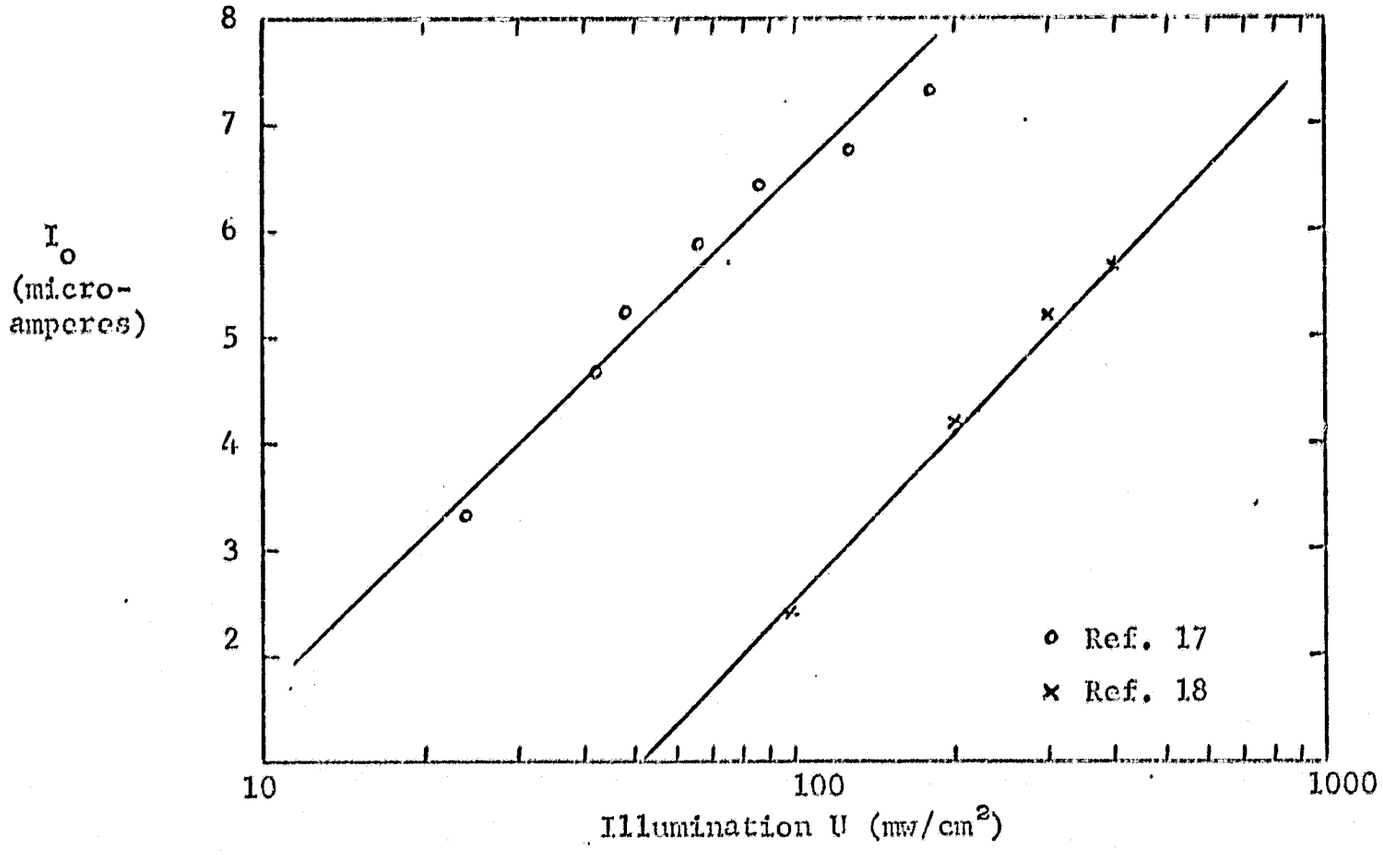

Figure 10. Plots of reverse saturation current I_o versus illumination intensity U. Laboratory data (refs. 17 and 18) were analyzed using Eq. 14.

The characteristic voltage V_o of the diode was explored in our previous report and appears to be independent of temperature, radiation exposure, and possibly illumination. For this reason, the expression AkT/q normally found in the solar cell equation, is replaced by a constant V_o in the mathematical model. This implies that A is inversely proportional to temperature, and measurements by Kennerud (ref. 8), replotted in Figure 11, show this. The lack of any clear dependence on radiation exposure is demonstrated in Figure 5.

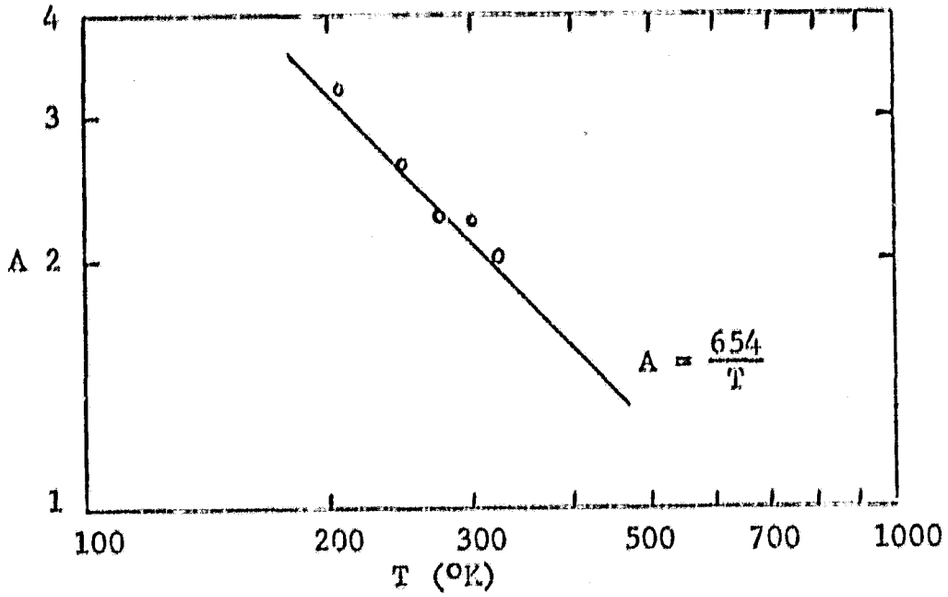

Figure 11. Reported values of A, versus temperature T, for typical n/p silicon solar cells. After reference 8.

D. Cell Resistance

The series resistance of a cell is seen from Figure 6 to increase with radiation exposure. Since this resistance R_s is a combination of many component resistances in series and parallel (ref. 9), quantitative prediction of the increase is difficult.

A significant portion of R_s is due to the sheet resistance of the surface region of the solar cell. Currents traveling from the junction along this thin layer to the grid lines are greatly affected by any change in its conductivity. Consequently, the major effect of radiation in increasing R_s appears to be through a decrease of the conductivity of the surface region.

A fit to the data in Figure 6 is

$$R_s = R_{so} \frac{1 + 1.5 \times 10^{-8} \langle K\Phi \rangle}{1 + 1.4 \times 10^{-8} \langle K\Phi \rangle} \tag{16}$$

where $\langle K\Phi \rangle$ is the damage integral, to be derived in Section III, and R_{so} is the initial resistance of the solar cell. This fit suggests that the initial resistance of the cell is entirely due to surface layer resistivity; the 100 keV protons could not have significant effect on the base region which they do not penetrate, nor on the metallic contacts.

II. OPTICAL EFFECTS

A. Coverslide Transmission

When sunlight strikes a solar cell assembly at an angle θ with the normal, it is partially transmitted through coverslide and into solar cell, and partially reflected at each of the interfaces. The transmitted light of wavelength λ moves through the coverslide at an angle ψ_λ with the normal; Snell's law gives this angle as

$$\cos \psi_\lambda = (m_\lambda^2 + \cos^2\theta - 1)^{\frac{1}{2}}/m_\lambda \tag{17}$$

where m_λ is the index of refraction of the coverslide. The angle θ_λ for transmission through the solar cell is likewise given by

$$\cos \theta_\lambda = (n_\lambda^2 + \cos^2\theta - 1)^{\frac{1}{2}}/n_\lambda \tag{18}$$

where n_λ is the index of refraction of silicon for wavelength λ. Further, for the components of unpolarized light, Fresnel's laws of reflection give the intensity of the reflected portion at each surface of the coverslide as

$$\beta_1(\|) = \left(\frac{-\sin(\theta - \psi_\lambda)}{\sin(\theta + \psi_\lambda)} \right)^2 \tag{19}$$

$$\beta_1(\perp) = \left(\frac{\tan(\theta - \psi_\lambda)}{\tan(\theta + \psi_\lambda)}\right)^2 \tag{20}$$

$$\beta_2(\parallel) = \left(\frac{-\sin(\psi_\lambda - \theta_\lambda)}{\sin(\psi_\lambda + \theta_\lambda)}\right)^2 \tag{21}$$

$$\beta_2(\perp) = \left(\frac{\tan(\psi_\lambda - \theta_\lambda)}{\tan(\psi_\lambda + \theta_\lambda)}\right)^2 \tag{22}$$

The transmitted light intensity through a coverslide with negligible absorption is then

$$t_\lambda = \frac{1}{2}\left\{\frac{[1 - \beta_1(\parallel)]\,[1 - \beta_2(\parallel)]}{1 - \beta_1(\parallel)\,\beta_2(\parallel)} + \frac{[1 - \beta_1(\perp)]\,[1 - \beta_2(\perp)]}{1 - \beta_1(\perp)\,\beta_2(\perp)}\right\} \tag{23}$$

Figure 12 presents calculated values of t_λ as a function of incident angle, for three representative values of n_λ, with the index of refraction m_λ of the coverslide equal 1.56. The two components of the unpolarized light are not transmitted equally at all angles, but the polarization of the transmitted light is of no importance to the present discussion. Furthermore, the magnitude of t_λ can be controlled to a considerable extent by the addition of so-called antireflective coatings. Eq. 21 shows the angular dependence of the light transmission probability, but underestimates the magnitude of t_λ when a proprietary optical coating is used. Experimental measurements of t_λ appear warranted for such a coverslide.

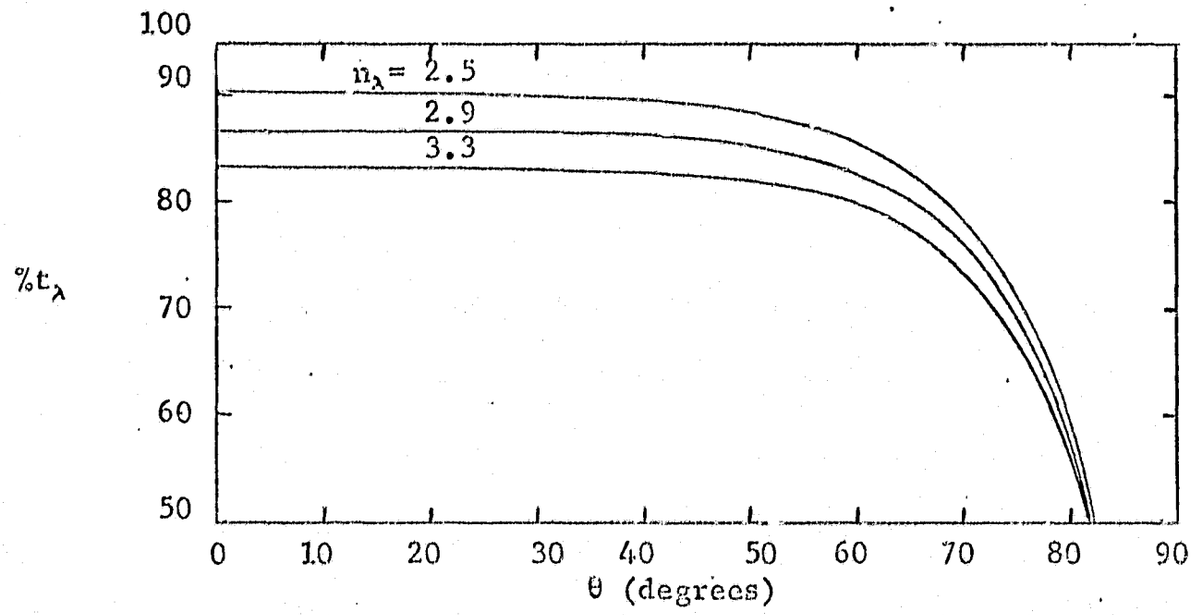

Figure 12. Ratio t_λ of the intensity of light entering the solar cell to light incident on the coverslide as a function of incidence angle θ.

Eq. 23 becomes indeterminate in the important case of perpendicular light incidence. For this case, the limiting form of t_λ is

$$t_\lambda = \frac{16\, m_\lambda^2\, n_\lambda}{(m_\lambda + 1)^2 (m_\lambda + n_\lambda)^2 - (m_\lambda - 1)^2 (m_\lambda - n_\lambda)^2} \tag{24}$$

B. Absorption in Silicon

In the solution of the difference equation (Eq. 8), the contribution to G(x) from different parts of the incident light spectrum must be considered. The source term is due to light within a range of wavelengths.

$$G(x) = \int_{\lambda_1}^{\lambda_2} G(x, \lambda)\, d\lambda \tag{25}$$

where λ_1 and λ_2 are the minimum and maximum wavelengths of sunlight to which the solar cell responds. These are normally taken as 0.4 and 1.1 microns.

Since no simple, closed form has been reported for the integral, G(x) may best be calculated using Simpson's Rule. The integrand is given by

$$G(x,\lambda) = \alpha(\lambda) H(\lambda) \left(\frac{\lambda}{\xi}\right) t_\lambda\, e^{-\alpha(\lambda)x} \tag{26}$$

Values of the absorption coefficient $\alpha(\lambda)$ and the spectral irradiance $H(\lambda)$ for space sunlight* are given in Table 1. The spectral irradiances are calculated for a sunlight intensity of 140 milliwatts per cm^2. The resultant G(x) is illustrated in Figure 13 for x up to .025 cm of silicon.

C. Coverslide Darkening

Absorption of light in a semitransparent material reduces the transmitted intensity to a fraction $e^{-\mu t/\cos\theta}$ where μ is an absorption coefficient, t is the slab thickness and θ is the angle of the slab perpendicular with the light ray in the material. Solar cell coverslides are

*Spectral irradiance may be defined as the differential of solar energy flux per unit wavelength. This is frequently depicted by Johnson's curve.

Table I

Absorption Coefficient of Silicon and Sunlight Intensity as a Function of Wavelength.

λ in microns, $\alpha(\lambda)$ in cm^{-1}

$H(\lambda)$ in watts/cm^2 -μ

λ	$\alpha(\lambda)$	$H(\lambda)$
0.40	7.50×10^4	0.1540
0.45	2.58×10^4	0.2200
0.50	1.18×10^4	0.1980
0.55	7.00×10^3	0.1950
0.60	4.65×10^3	0.1810
0.65	3.33×10^3	0.1620
0.70	2.42×10^3	0.1440
0.75	1.69×10^3	0.1270
0.80	1.12×10^3	0.1127
0.85	7.95×10^2	0.1003
0.90	3.80×10^2	0.0895
0.95	1.80×10^2	0.0803
1.00	7.30×10^1	0.0725
1.05	2.08×10^1	0.0665
1.10	4.40×10^0	0.0606

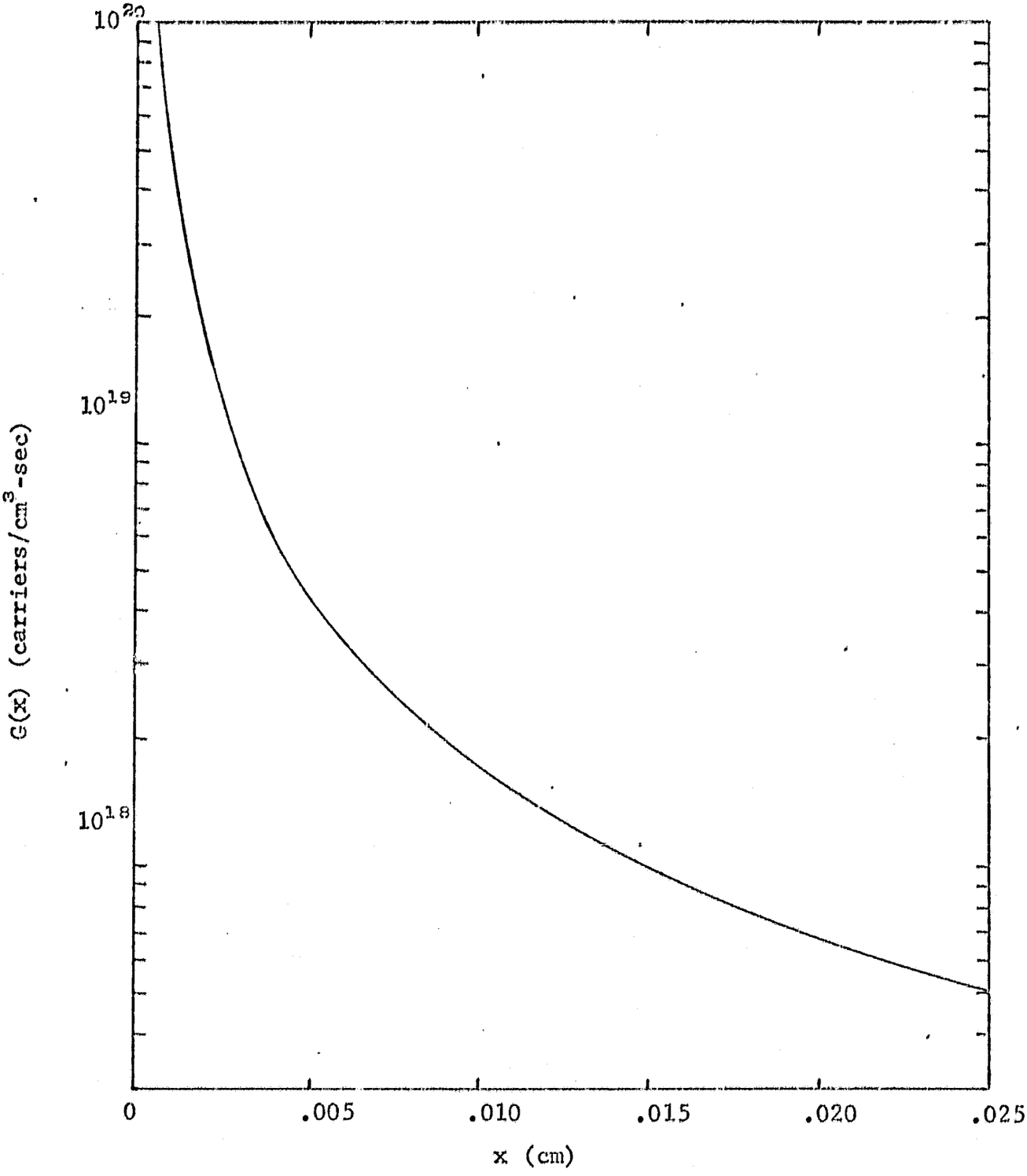

Figure 13. Computed values of the number of minority carriers/ cm^3-sec produced in silicon by space sunlight as a function of depth x of penetration. Values from Table 1 were used in equation 26 and reflection was neglected.

sufficiently clear and thin so that initially the absorption coefficient is essentially zero. Furthermore, measurements indicate for silica coverslides that extremely large electron fluences, on the order of 10^{16} or more, are required to reduce the transmission by about 2% (ref. 14).

Darkening due to radiation degradation of any antireflective coatings on the coverslide, and of adhesive between coverslide and solar cell may be more severe. A quantitative evaluation of this darkening depends on measurements of the specified coverslide assembly before and after irradiation in vacuum. Protons, electrons, and ultraviolet radiation should be considered.

III. RADIATION EFFECTS

A. Proton Shielding

The thickness of a solar cell is comparable to the distance a proton can travel in silicon when its energy is typical of protons found in space. Shielding by a coverslide and self-shielding by the solar cell are consequently important. This is especially significant when one considers the proton energy-dependence of damage.

The distance of travel, or range R, is often related to the incident proton energy E_o by formulas of the form

$$R = R_o E_o^n \tag{27}$$

The equation is not exact, but good fits can be provided over limited ranges of E_o. Table 2 is such a fit to tabulated data.

Table 2

Values of R_o and n for proton range-energy relationships and corresponding energy intervals.*

Energy (MeV)	R_o (mg/cm^2)	n
$0.0 \leq E < 0.3$	2.81	0.995
$0.3 \leq E < 0.8$	3.945	1.277
$0.8 \leq E < 2.0$	4.11	1.460
$2.0 \leq E < 200$	3.42	1.726

*computed from data in ref. 10

The range formula implies that the energy of a proton along its track can be calculated from the residual distance it is to travel before stopping. The relation is not exact, for there is some straggling of the individual tracks of protons of the same energy, but it is generally quite small. The average straggling, as a fraction of R, decreases with proton energy E_o and it is less than 4% for 100 keV protons (ref. 10). Thus, we treat the range equation as being exact and compute a proton energy $\left(E_o^n - \frac{X}{R_o}\right)^{1/n}$ for protons of initial energy E_o which have traveled a distance X in silicon. When monoenergetic protons of an omnidirectional fluence strike the solar cell surface, the effects of slant penetration cause a spectrum at depths X.

A coverslide of thickness a will remove protons of energy E_o and incident angle θ with the normal if their range R is less than the path length $a/\cos\theta$ through the coverslide. It will also reduce the energy of a transmitted proton to E given by[13]

$$E = \left[E_o^{\,n} - \frac{a}{R_o \cos\theta}\right]^{1/n} \tag{28}$$

where R_o may be taken as 2.72 mg/cm^2 when n is 1.75.

The proton spectrum striking the solar cell due to a monoenergetic, unit flux incident isotropically on the coverslide can be obtained. The result is

$$\Phi(E) = \frac{naE^{n-1}}{R_o(E_o^n - E^n)^2} \qquad \text{For } E < E_o \tag{29}$$

Superposition of this result yields the proton spectrum $\Phi(E)$ incident on the solar cell due to an isotropic fluence $\Phi(E_o)$ in space penetrating a shield of thickness t, expressed in mass per unit area. The proton fluence at depth z in the solar cell assembly is related to the proton fluence $\Phi_p(E_o)$ in space by

$$\Phi_p(E,z) = nz \sum_{E_o > E_c} \left(\frac{\Phi_p(E_o)\, E^{n-1}}{R_o \left[E_o^{\,n} - E^n\right]^2} \right) \tag{30}$$

Sufficiently small energy increments for the tabular input of the incremental fluences in space should be chosen so that the summation approaches an integral.

The shielding effect by a coverslide and by the silicon is proportional to the product of density and thickness. Therefore, X should be given in mass per cm^2 in calculations of shielding.

B. Proton Damage

The proton damage coefficient K_p is the measure of decreases in minority carrier diffusion length due to a fluence Φ of protons (K_p equals the incremental increase in the quantity $1/L^2$ with incremental increase in Φ). The damage is due to Rutherford scattering of protons, which dislodges silicon atoms from their lattice position. Hence, the proton energy dependence of K_p is approximately given by $1/E$, which is the energy dependence of the Rutherford scattering cross section. The threshold for dislodging atoms corresponds to a minimum proton energy of about 0.0001 MeV.

Crowther et al (ref. 11) have found a flattening of the energy dependence of K_p below about 0.5 MeV. This effect, seen in Figure 14, may correspond to an annealing mechanism whereby a dislodged atom has not been pushed far from its site, and has a high probability of return. The following equations fit these measurements for 1 ohm-cm p-silicon and provide a ratio for higher resistivity p-silicon that agrees with measurements by Denney and Downing (ref. 12).

$$K_p(E) = 1.2\,\Omega^{-0.75}\,E^{-0.9} \times 10^{-5} \qquad [E > 3\ \text{MeV}] \qquad (31)$$

$$K_p(E) = 1.92\,\Omega^{-0.75}\,e^{-1.04}(E/.962)^{-0.85} \times 10^{-5} \qquad [3 > E > 1] \qquad (32)$$

$$K_p(E) = 1.92\,\Omega^{-0.75}\,e^{-1.08E} \times 10^{-5} \qquad [1 > E > 10^{-4}] \qquad (33)$$

Because proton energy changes rapidly with depth of penetration into the cell, and because the damage coefficient K_p is so dependent on proton energy, damage by protons of less than about 5 MeV results in a highly nonuniform minority carrier diffusion length across the cell.

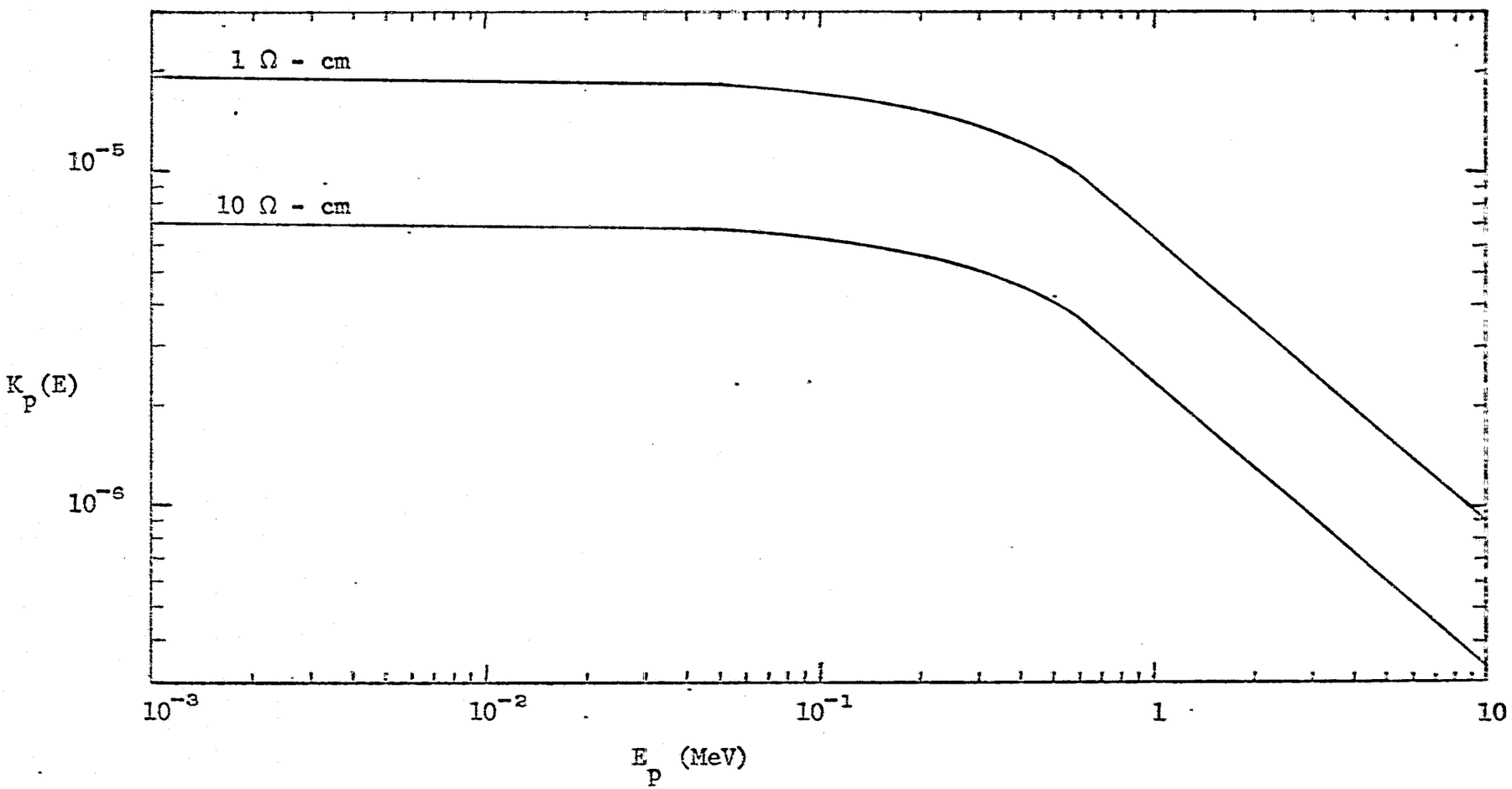

Figure 14. Proton damage coefficient for 1 and 10 Ω-cm p-type silicon versus proton energy illustrating the flattening of the energy dependence of K below 0.5 MeV.

Through the continuity equation, this results in a large fluctuation in minority carrier distribution. As an example, we have used these values of K and proton range R to calculate the minority carrier distribution in the bare cells Statler and Curtin irradiated with 270 keV protons. The minority carrier distribution is shown in Figure 15 for various exposures to the proton fluence Φ.

C. Electron Shielding

The spectrum of electrons at various depths from an irradiated surface has been studied by numerous workers. The problem is complicated by Rutherford scattering: electrons collide with atomic nuclei and may make a sharp change of direction and energy. As a result, a beam of electrons that was initially monoenergetic assumes a spectrum of energies that changes with depth of penetration. There is no unique range for electrons such as there is for protons.

To determine the portion of the damage integral due to electrons, it is necessary to know a function $y(E, E_o, X)$ which gives the probability that an electron of energy E_o striking the coverslide will penetrate to a depth given by X and have an energy E at that depth. This function, when multiplied with the spectrum of the incident electrons, will then provide the spectrum of the electrons as they penetrate the coverslide and the solar cell. To be applied to calculations of irradiation in space, the function should be appropriate to an omnidirectional electron flux.

Some characteristics the function $y(E, E_o, X)$ must have are readily seen. Since $y(E, E_o, X)$ times the incident flux equals the flux at depth X, then it must become a delta function in $(E-E_o)$ for limit of X equal zero. The second obvious characteristic required of our function is that it should vanish not only for E greater than E_o, but for E greater than E_o less the energy loss for an electron penetrating directly to the depth X without a single Rutherford collision. Finally, the function should approach zero as X approaches the range of the electrons.

A function with these characteristics was derived by a graphical analysis of Monte Carlo data (ref. 13) for monoenergetic, isotropic electron

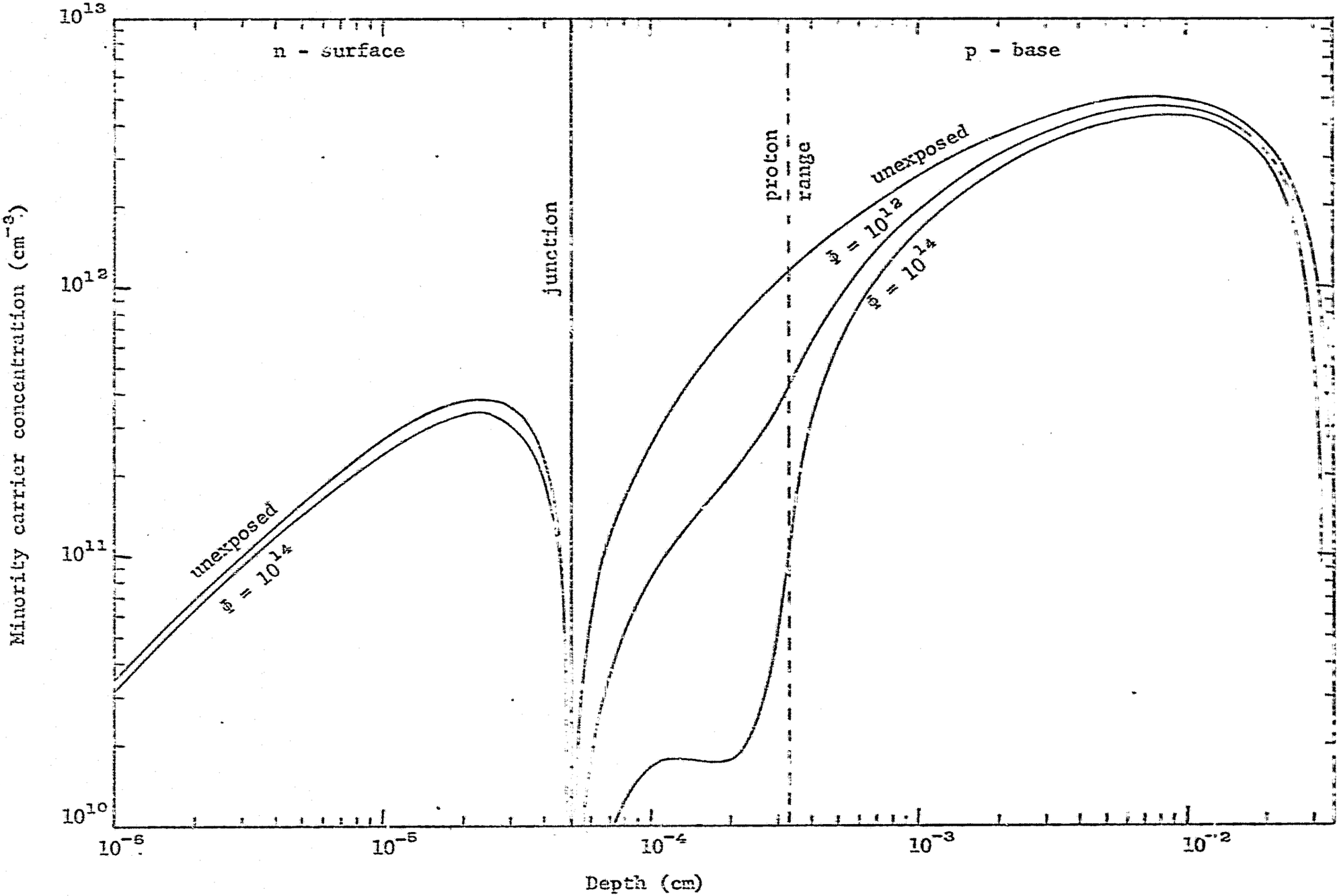

Figure 15. Calculated minority carrier concentration versus depth in a silicon n/p solar cell before and after exposure to non-penetrating protons, of 270 keV energy.

fluences. These data had been generated in terms of the path length P (which is the slowing down integral). Therefore, E_o was related to P by an empirical fit.

The fit to P, with error less than 3% for electron energies up to 6 MeV is

$$P = \frac{0.7\ E_o^{1.98}}{0.29 + E_o} \tag{34}$$

With the dimensionless depth t

$$t = (a + X_k \rho)/P \tag{35}$$

the functional dependence of the electron fluence at depth t on the electron fluence incident on the solar cell assembly is

$$\Phi_e(E, X_k) = \sum_{E_o} \frac{\Phi_e(E_o)\ (1.0 + 7.0t)\ (c_1/t)\ e^{(c_1/tE_o)(E-E_o)}}{c_2 + e^{c_3(E/E_o)-c_4} + e^{c_5(c_6 - E/E_o)}} \tag{36}$$

Where the parameters are given by

$$c_1 = 0.65 - .03E_o + 3.6t \tag{37}$$

$$c_2 = 1 + \left(2.4t^3/\sqrt{E_o}\right) \tag{38}$$

$$c_3 = \left(6.7\sqrt{E_o}/t^{1.6}\right) + 5 \tag{39}$$

$$c_4 = c_3\ (1.04 - .012\ \ell n\ E_o)\ (1-t) \tag{40}$$

$$c_5 = 30t^2 + 0.7 \tag{41}$$

$$c_6 = 0.3 - (.02/t^2) \tag{42}$$

D. Electron Damage

The damage coefficient K_e for electron damage in p-type silicon has been fitted empirically by a formula shown in Figure 16. We neglect

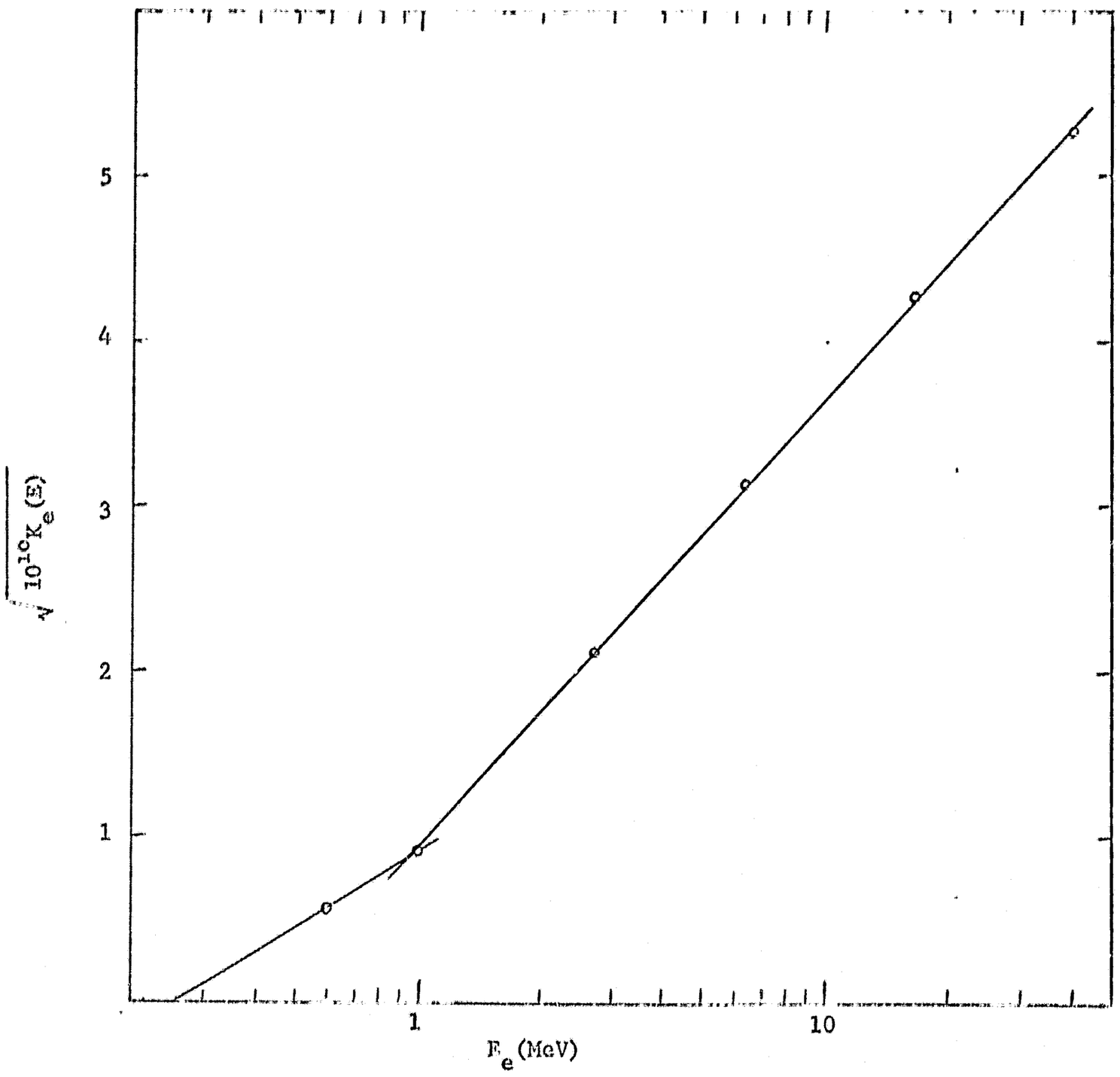

Figure 16. A plot of the square root of the electron damage coefficient versus electron energy. (Data points for p-type silicon, having a resistivity of 10.6 ohm cm, from ref. 19.)

to study fits for n-type silicon since electron damage is negligible in the surface region, compared to that in the base region. We plotted the square root of measured values of K_e versus electron energy. For crucible-grown p-type silicon of resistivity 10.6 ohm-cm, the points, shown in Figure 15, can be connected by two straight line segments. That a straight line results over the energy range 1-40 MeV indicates that a recombination center requiring two defects may be involved (ref. 20). Below 1 MeV, sufficient data are not available for such a conclusion, but a straight line curve fit can be presented.

This fitting of the data, and the dependence on electrical resistivity discussed above, give the damage coefficient as

$$K_e(E) = (10/\Omega)^{0.5} \; (1.2\,\ell n 2.17E)^2 \times 10^{-10} \qquad [E > 1\ \text{MeV}] \qquad (43)$$

$$K_e(E) = (10/\Omega)^{0.5} \; (0.67\,\ell n 4E)^2 \times 10^{-10} \qquad [1 > E > .25] \qquad (44)$$

$$K_e(E) = 0 \qquad [.25 > E] \qquad (45)$$

where Ω is the resistivity in ohm-centimeters and E is the electron energy in MeV. The expression to fit measurements between 1 and 40 MeV will underestimate the damage for lower energies. Below 1 MeV, the second factor in the equation can be replaced by $(0.67\ \ell n 4E)^2$. This fits the measurement at 0.6 MeV and the generally observed "apparent" threshold of 250 keV. The damage integral can now be evaluated at each depth X_k.

$$\langle K\Phi \rangle_k = \sum K_p(E)\,\Phi_p(E,X_k) + \sum K_e(E)\,\Phi_e(E,X_k) \qquad (46)$$

IV. RECOMMENDED FUTURE WORK

A. Low Energy Proton Damage

The parameter I_L has repeatedly been shown to be strongly dependent on the minority carrier diffusion length in the base of solar cells. While this relationship has become a textbook exercise (ref. 4), surprisingly little work has been done on the case where the diffusion length varies

with depth into the cell. This, however, would be normal when cells are exposed low energy protons such as predominate in high orbits and in some solar flares. We have presented a mathematical technique to evaluate I_L under uniform or nonuniform damage, based on the existing theory.

For solar cells that have been uniformly damaged, the technique works quite well, as evidenced in Figure 17. No normalization factor was necessary for the excellent agreement shown between the model calculations and the reported measurements. This would indicate that the model equations correctly reproduce the effects of cell thickness, the nonlinearity of absorption of space sunlight, the magnitude of the degraded minority carrier diffusion length, and the relation between photovoltaic current and minority carrier concentration.

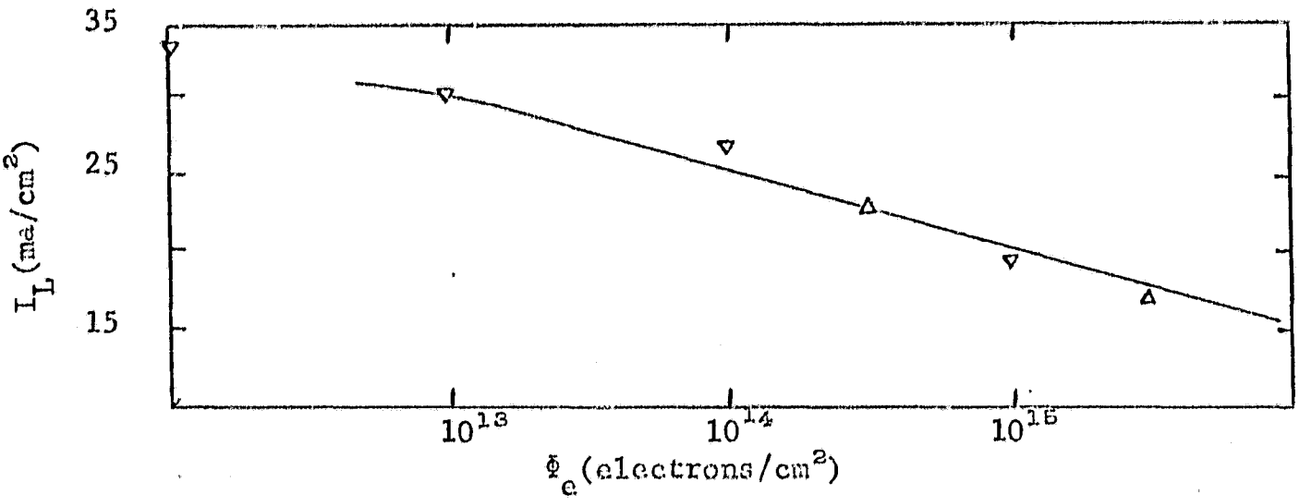

Figure 17. Photovoltaic current (milliamperes/cm^2) versus fluence of 1 MeV electrons (Exp. by Denney Δ and by Carter ∇)

At present, difficulty is being encountered in relating for solar cells which have been damaged by protons which do not penetrate the cell completely. The accepted relationships found in the literature do not generate correct solutions for this problem. We can avoid the difficulty by postulating a very low value for damage effectiveness of low energy protons. However, the value to be chosen is in disagreement with theoretical evaluations of the energy dependence of proton damage. An extended analysis of proton damage appears warranted, to insure that the predictions of the model are acceptable when large amounts of low energy proton damage occur.

In the past, damage to solar cells by low energy protons has been treated in a loose manner. The decrease in a cell parameter, often the short-circuit current, has been measured against the fluence of protons causing it. Knowing these, one can develop an effective damage coefficient, to relate the two and use this parameter in equations of uniform damage relationships. Since the effective parameter is selected to force the correct value of the short-circuit current, the mathematics generally work. The situation to be investigated must not differ greatly from the experiment used to generate the parameters. Otherwise, there is no guarantee of accuracy since the procedure is obviously of the ad hoc type.

The development of a technique to relate low energy proton damage to short-circuit current has allowed a more precise analysis. Instead of an effective damage coefficient, a true damage coefficient can be reproduced in the mathematics. Doing this, we have found that the theoretical expressions overestimate the actual damage in the cases we have analyzed. The results we have obtained are shown in Figure 18. Several possibilities exist to explain why low energy protons are not as damaging as predicted.

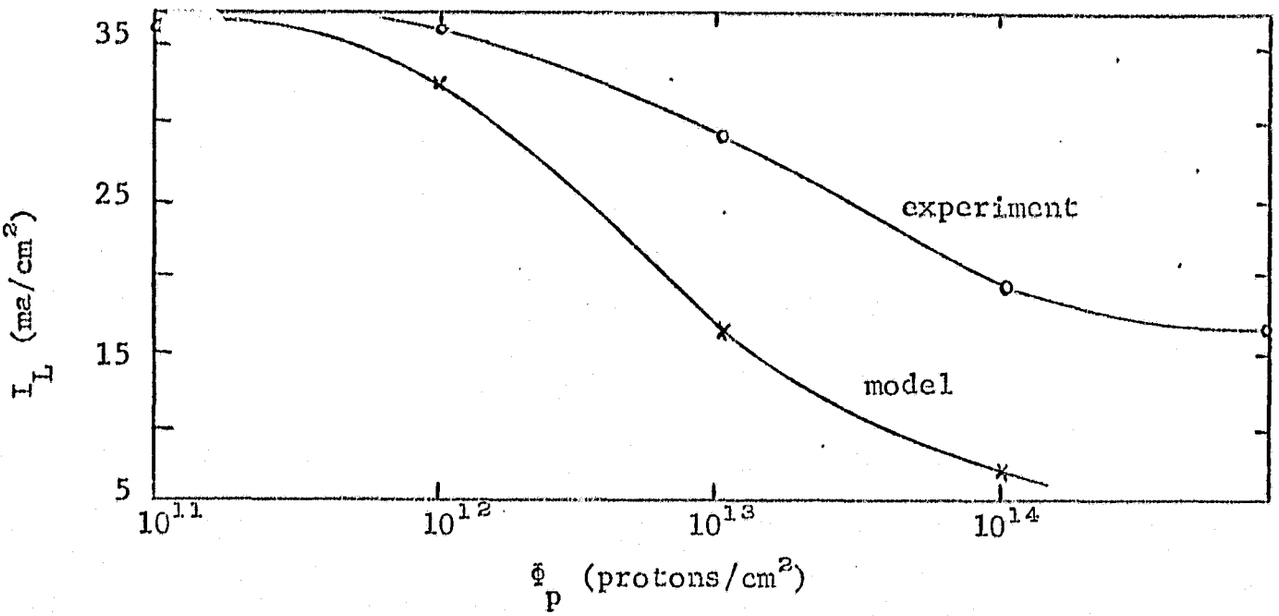

Figure 18: Photovoltaic current (milliamperes/cm^2) versus fluence of 270 keV protons (Exp. by Statler and Curtin)

The first possibility that one might consider here is the interference between defects at the end of the track of the proton. Each proton produces about 5×10^5 displacements/cm as it is slowed down from an energy of 10 keV to 1 keV. Conceivably, in a large fluence of protons, many of the collisions that occur could be with silicon atoms that have already been displaced. These can not be counted as additional defects. Assuming that all silicon atoms, whether displaced or in lattice positions, are equally likely to be struck by a proton, we estimate that this interference should be significant when the proton fluence is of the order of $10^{17}/cm^2$.

The deviation between theory and measurement occurs much lower, around fluences of the order of $10^{12}/cm^2$. However, the assumption made may be in error; the displaced silicon atoms could be more likely to be struck than are the lattice atoms. This would be a channeling effect, whereby lattice atoms, particularly those at the end of the proton track, shadow each other to reduce a collision probability. This needs a more detailed theoretical investigation.

Another possibility is that displacements occur and interfere with each other. A lattice vacancy, according to theory, diffuses through the lattice until it finds a stable configuration. One such configuration is a recombination center, which is electrically active in reducing the

ity. Another configuration, of course, would be a vacancy filled with a silicon that had been interstitial. This would be electrically inactive, and be readily evaluated in terms of theory.

A third possibility for investigation takes into account the proton, or hydrogen atom, that is left at the end of the track. The proton could combine either with a vacancy or with a recombination center to reduce its damage effectiveness. This would be a form of annealing, perhaps similar to that noted with lithium. (These atoms are similar, having the same valence, and similar size.) That annealing of up to 90% of the defects does occur has already been noted (ref. 6).

Finally, the recombination center may persist but be incorrectly evaluated. The current study does not include evaluation of fill factors,

which are known to be significantly affected by illumination intensity. This topic has recently been of concern and is the subject of current investigations elsewhere. The results should be incorporated in the mathematical model and computer program. It is known that fill factor for proton-induced recombination centers is a function of light intensity (ref. 1). Even if we restrict ourselves to a one-sun-intensity model, suitable only for near-Earth orbits, this function can be important. This is because light is strongly attenuated in silicon. The light intensity at the recombination center is therefore a function of its distance from the surface of the cell.

B. Resistance Effects

Radiation damage reduces both the charge carrier concentration and mobility. These reduction combine to increase the resistivity of n and p silicon with exposure to radiation. Future work is needed to establish the quantitative nature of this increase. Whether the nature of the dopant affects the change, whether it is linear with exposure, whether temperature plays a significant role, and whether the nature of the damage depends on the bombarding particle, are questions to be answered by such work.

The series resistance of a solar cell is a composite of resistance terms due to current flow across the bulk region, along the surface region to the contacts, and across from silicon to front and back contacts. Each of these terms logically would behave differently under radiation exposure. As a consequence, careful analysis of resistance effects would require one first to partition R_s among its components, and then scale these components as they change with radiation exposure. Some uncertainty is obvious in this scheme (even if the effect of radiation on silicon resistivity were known), since manufacturing tolerances would vary the components from cell to cell. Finally, catastrophic events such as the lifting of a contact would be difficult to predict. This would lead to a value of R_s much greater than normally expected; Figure 6 shows such a value.

Fortunately, cell resistance plays a small part in the behavior of a solar cell. An empirical formula such as Eq. 16 for an estimate may be generally satisfactory. More experimental measurements would be useful in

improving the estimate and it is puzzling that such measurements have not been reported.

V. GLOSSARY

English letters

a	thickness of coverslide (gms/cm^2)
b	thickness of the solar cell (cm)
D	diffusion coefficient for minority carriers (cm)
d	darkening coefficient (to be measured experimentally for coverslide with antireflective coatings and adhesive)
E	electric field in cell, due to impurity gradient (volts/cm)
E, E_k	energy of a particle in a solar cell (MeV)
E_c	energy of a proton which has a range X (MeV)
E_o	energy of a particle incident on a solar cell (MeV)
e	base of natural logarithms: 2.72
f	fraction of front surface of solar cell not covered by contact
G_k	rate of production of minority carriers per cm^3 at depth X_k in silicon (carriers/cm^3-sec)
H_λ	spectral irradiance outside solar cell assembly, at wavelength λ (watts-cm^2-micron)
I	current from a solar cell (amperes)
I_o	diode reverse-saturation current of a solar cell (amperes)
I_{oo}	initial diode reverse - saturation current (amperes)
I_L	photovoltaic current induced in a solar cell (amperes)
I_{sc}	current from a short-circuited solar cell (amperes)
j	photovoltaic current density (amps/cm^2)

K_p, K_e	damage coefficient relating proton or electron fluence and decrease in L (dimensionless)
$\langle K\Phi \rangle_k$	damage integral, evaluated at X_k
k	Stefan-Boltzmann constant: 1.38×10^{-23} joule/molecule ^oK
L_b	base minority carrier diffusion length before irradiation (cm)
L_k	minority carrier diffusion length (cm) at X_k
L_s	surface minority carrier diffusion length before irradiation (cm)
m_λ	index of refraction of glass for light of wavelength λ
n	parameter from Table 1 for proton range
n_k	minority carrier concentration at depth X_k (carriers/cm^3)
n_λ	index of refraction of silicon for light of wavelength λ
P	electron slowing down integral: length of track traveled by an electron in silicon before it loses its initial energy
q	unit electrical charge: 1.6×10^{-19} coulombs
R_L	resistance of load across solar cell (ohms)
R_o	parameter from Table 1 for proton range
R_s	series resistance of solar cell (ohms)
R_{so}	series resistance of cell before radiation exposure (ohms)
S	front surface area of the solar cell (cm^2)
T	absolute temperature (degrees Kelvin)
t	depth X_k in units of electron slowing down integral P $\quad t = (a + X_k\rho)/P$

t_λ — ratio of intensity of light entering solar cell to light incident on coverslide, for wavelength λ

U — light intensity incident on solar cell assembly (milliwatts/cm^2)

$\frac{dU}{d\lambda}$ — differential energy spectrum of light source (watts/cm^2-micron)

V_o — characteristic voltage of solar cell (volts) ($V_o = AkT/q$)

V_{oc} — potential across an open-circuited solar cell (volts)

$$V_{oc} = V_o \ln\left(1 + \frac{I_L}{I_o}\right)$$

X_j — depth of junction below surface of solar cell (cm)

X_k — distance from outer surface of coverslide (cm)

Z — depth of penetration (ξms/cm^2) $Z = a + X_k \rho$

Greek Letters

α — absorption coefficient in silicon for light of wavelength λ (cm^{-1})

$\beta_1(\parallel), \beta_1(\perp)$ — ratio of amplitude of reflected light to incident light at space/coverslide interface for polarized light

$\beta_2(\parallel), \beta_1(\perp)$ — same as above, but at coverslide/silicon interface

β — probability of reflection from the solar cell-coverslide assembly for light of wavelength λ

Δ — mesh interval: distance between X_k and X_{k+1} (cm)

$\Delta\lambda$ — increment of wavelength (microns)

θ — angle between a perpendicular to the solar cell surface and the direction of the sun (degrees)

θ_λ — angle of light ray in silicon, having angle θ in space with respect to normal and wavelength λ (degrees)

λ — wavelength of light (microns)

ξ — Planck's constant times the speed of light $\xi = 1.99 \times 10^{-23}$ watt-cm-sec

τ	mean lifetime of a minority carrier in the conduction band (sec)
μ	minority carrier mobility (cm^2/volt-sec)
ρ	density of silicon (2.33 grams/cm^3)
$\Phi_p(E_o)$	protons/cm^2-MeV about an energy E to which the solar cell assembly has been exposed
$\Phi_e(E_o)$	electrons/cm^2-MeV about an energy E to which the solar cell assembly has been exposed
ψ_λ	angle of light ray in glass, having incident angle θ (degrees)
Ω	resistivity of solar cell base region (ohm-cm)

VI. REFERENCES

1. Wolf, M. and Prince, M. B.: "New Developments in Silicon Photovoltaic Devices and Their Application to Electronics", Proceedings of the International Conference in Brussels 2-7 June, 1958.

2. Lodi, E.: "Lockheed Low-Energy Proton Damage Experiments." Transcript of the Photovoltaic Specialists Conference. Vol. I, Section B-4. July 1963.

3. Statler, R. L. and Curtin, D. J.: "Low Energy Proton Damage in Partially Shielded and Fully Shielded Silicon Solar Cells." Communications Satellite Corporation Technical Memorandum CL-24-68. November 1968. (additional information by private communication)

4. Brown, W. D.: "ATS Power Subsystems Radiation Effects Study." Phase I/ Final Report on NASA Contract NAS5-3823. February 1968.

5. Shockley, W.: Bell Syst. Tech. J. 28, 435 (1949).

6. Downing, R. G.: "Low Energy Proton Degradation in Silicon Solar Cells." Proc. of the 5th Photovoltaic Specialists Conference, Vol. II, Section D-7, January 1966.

7. Luft, W.: "Effects of Electron Irradiation on N on P Silicon Solar Cells." Advanced Energy Conversion. Vol. 5, pp. [illegible] 65.

8. Kennerud, K. L.: "Electrical Characteristics of Silicon Solar Cells at Low Temperatures" IEEE Trans. Aerospace & Elec. Sys. AES-3. July 1967.

9. Handy, R. J.: "Theoretical Analysis of the Series Resistance of a Solar Cell." Solid State Electronics, Vol. 10, pp. 765-775. March 1967.

10. Janni, J. F.: "Calculations of Energy Loss, Path Length, Straggling, Multiple Scattering, and the Probability of Inelastic Collisions for 0.1 to 1000 MeV Protons." Air Force Weapons Laboratory. Technical Report No. AFWL-TR-65-150. September 1966.

11. Crowther, D. L., et. al: "An Analysis of Nonuniform Proton Irradiation Damage in Silicon Solar Cells". IEEE Trans. on Nuclear Sciences NS-13: No. 5, 37-49. October 1966.

12. Denney, J. M. and Downing, R. G.: "Charged Particle Radiation Damage in Semiconductors, IX: Proton Radiation Damage in Silicon Solar Cells." TRW Space Technology Labs., Redondo Beach, Calif., Final Report on Contract NAS5-1851. TRW 8653-6026-KU-000. August 1963.

13. Lopez, M.: (NASA Manned Space Flight Center), private communication, of Monte Carlo calculations using a code written by M. Berger and S. Seltzer of Nat. Bureau of Standards.

14. Campbell, F. J.: "Effects of Radiation on Transmittance of Glasses and Adhesives." Presented at the 17th Annual Power Sources Conference, May 21-23, 1963. (Sponsored by NASA and the Dept. of the Navy)

15. Tada, H. Y.: "A Theoretical Model for Low-Energy Proton Irradiated Silicon Solar Cells." Proceedings of the 5th Photovoltaic Specialists Conference, Vol. II. January 1966.

16. Bullis, M. W., and Runyan, W. R.: "Influence of Mobility Variations on Drift Field Enhancement in Silicon Solar Cells." Appendix to NASA Report CR-461. Prepared under NASA Contract No. NAS5-3559.

17. Brown, W. D., et al: "Computer Simulation of Solar Array Performance." In Proc. of the 6th Photovoltaic Specialists Conference, Vol. II, 233-250. March 1967.

18. Wolf, Martin, and Hans Rauschenbach: "Series Resistance Effects on Solar Cell Measurements." Advanced Energy Conversion. Vol. 3, pp 455-479. Pergamon Press, 1963.

19. Denney, J. M., et al: "The Energy Dependence of Electron Damage in Silicon." 4141-6004-KU-000, TRW Space Tech. Laboratories, September 1964.

20. Barrett, M. J.: "Electron Damage Coefficients in P-Type Silicon." IEEE Trans. on Nuc. Sci. No. 6, December, 1967.

VII. NEW TECHNOLOGY

After a diligent review of the work performed under this contract, no new innovation, discovery, improvement or mention was made.

APPENDIX: COVERSLIDE TRANSMISSION AT NORMAL INCIDENCE

The transmitted light intensity through a coverslide with negligible absorption is given by equation 23 where $\beta_1(\parallel)$, $\beta_2(\parallel)$, $\beta_1(\perp)$, and $\beta_2(\perp)$ are given by equations 19 through 22. In the case of normal incidence where θ, ψ_λ, and θ_λ all equal zero, direct substitution yields an indeterminate solution. However, since the tangent approaches the sine at small angles we have

$$\beta_1(\parallel) = \beta_1(\perp) = \left[\frac{-\sin(\theta - \psi_\lambda)}{\sin(\theta + \psi_\lambda)}\right]^2 = \left[\frac{-\sin\theta\cos\psi_\lambda + \cos\theta\sin\psi_\lambda}{\sin\theta\cos\psi_\lambda + \cos\theta\sin\psi_\lambda}\right]^2 \qquad (47)$$

and

$$\beta_2(\parallel) = \beta_2(\perp) = \left[\frac{-\sin(\psi_\lambda - \theta_\lambda)}{\sin(\psi_\lambda + \theta_\lambda)}\right]^2 = \left[\frac{-\sin\psi_\lambda\cos\theta_\lambda + \cos\psi_\lambda\sin\theta_\lambda}{\sin\psi_\lambda\cos\theta_\lambda + \cos\psi_\lambda\sin\theta_\lambda}\right]^2 \qquad (48)$$

Dividing numerator and dinominator of the first equation by $\sin\psi_\lambda$ and of the second equation by $\sin\theta_\lambda$, and replacing $\sin\theta/\sin\psi_\lambda$ by m_λ and $\sin\psi_\lambda/\sin\theta_\lambda$ by n_λ/m_λ from Snell's law the equations reduce to

$$\beta_1(\parallel) = \beta_1(\perp) = \left(\frac{-m_\lambda + 1}{m_\lambda + 1}\right)^2 \qquad (49)$$

and

$$\beta_2(\parallel) = \beta_2(\perp) = \left(\frac{-m_\lambda + n_\lambda}{m_\lambda + n_\lambda}\right)^2 \qquad (50)$$

Substitution of these quantities into equation 23 and simplification yield equation 24.